



Published in final edited form as:

Arterioscler Thromb Vasc Biol. 2014 January ; 34(1): 26–33. doi:10.1161/ATVBAHA.113.302355.

Acceleration of Biliary Cholesterol Secretion Restores Glycemic Control and Alleviates Hypertriglyceridemia in Obese *db/db* Mice

Kai Su*, Nadezhda S. Sabeva*, Yuhuan Wang, Xiaoxi Liu, Joshua D. Lester, Jingjing Liu, Shuang Liang, and Gregory A. Graf

Department of Pharmaceutical Sciences, Graduate Center for Nutritional Sciences and Saha Cardiovascular Research Center, University of Kentucky, Lexington (K.S., Y.W., X.L., J.D.L., G.A.G.); Department of Neuroscience, Universidad Central del Caribe, Bayamon, Puerto Rico (N.S.S.); Department of Molecular Genetics, University of Texas Southwestern Medical Center, Dallas (J.L.); and Department of Clinical Laboratories, Jinshan Branch of the Sixth People's Hospital of Shanghai, Shanghai, China (S.L.)

Abstract

Objective—Recent studies support a role for cholesterol in the development of obesity and nonalcoholic fatty liver disease. Mice lacking the ABCG5 ABCG8 (G5G8) sterol transporter have reduced biliary cholesterol secretion and are more susceptible to steatosis, hepatic insulin resistance, and loss of glycemic control when challenged with a high-fat diet. We hypothesized that accelerating G5G8-mediated biliary cholesterol secretion would correct these phenotypes in obese mice.

Approach and Results—Obese (*db/db*) male and their lean littermates were administered a cocktail of control adenovirus or adenoviral vectors encoding ABCG5 and ABCG8 (AdG5G8). Three days after viral administration, measures of lipid and glucose homeostasis were determined, and tissues were collected for biochemical analyses. AdG5G8 increased biliary cholesterol and fecal sterol elimination. Fasting glucose and triglycerides declined, and glucose tolerance improved in obese mice expressing G5G8 compared with mice receiving control adenovirus. These changes were associated with a reduction in phosphorylated eukaryotic initiation factor 2 α and c-Jun N-terminal kinase in liver, suggesting alleviation of endoplasmic reticulum stress. Phosphorylated insulin receptor and protein kinase B were increased, indicating restored hepatic insulin signaling. However, there was no reduction in hepatic triglycerides after the 3-day treatment period.

Conclusions—Accelerating biliary cholesterol secretion restores glycemic control and reduces plasma triglycerides in obese *db/db* mice.

© 2013 American Heart Association, Inc.

Correspondence to Gregory A. Graf, PhD, Pharmaceutical Sciences, University of Kentucky, Room 345 Biopharmaceutical Complex, 789 S Limestone, Lexington, KY 40536-0082. Gregory.Graf@uky.edu.

*These authors contributed equally.

The online-only Data Supplement is available with this article at <http://atvb.ahajournals.org/lookup/suppl/doi:10.1161/ATVBAHA.113.302355/-/DC1>.

Disclosures

None.

Keywords

bile; cholesterol; insulin resistance; liver steatosis; obesity

The causal role of cholesterol in the development of cardiovascular disease is well-established, but an emerging body of literature indicates that cholesterol may also contribute to the development of obesity and the severity of nonalcoholic fatty liver disease (NAFLD). Dietary cholesterol and fat act synergistically to promote obesity and the development of NAFLD in C57BL6/J mice.¹ Similarly, the addition of cholesterol to a high-fat, high-sucrose diet also exacerbates the development of insulin resistance and steatosis in low-density lipoprotein receptor (LDLR)-deficient mice.² In a mouse model of Alström syndrome, hepatic cholesterol accumulation is associated with disruptions in both cholesterol uptake and elimination pathways and correlates with the severity of liver phenotypes.³ Conversely, the inhibition of cholesterol absorption with ezetimibe (EZ) opposes the development of obesity, insulin resistance, and steatosis in both rats and mice.⁴⁻⁷ Mice lacking the target of EZ, Niemann-Pick C1-like 1 protein, are protected from NAFLD and the development of obesity and insulin resistance.⁸⁻¹⁰ However, the addition of cholesterol to the diet reverses this phenotype, suggesting that the presence of cholesterol in the intestine modulates metabolism independently of its absorption.¹¹ In the LDLR model challenged with a high-cholesterol diabetogenic diet, EZ reduced hepatic steatosis but not other obesity phenotypes such as adipose tissue inflammation.¹² EZ was shown to produce a modest, but significant, reduction in hepatic fat and liver enzymes in a Japanese population of patients with NAFLD.¹³ In addition, a recent clinical trial suggests that EZ may improve measures of insulin resistance in diabetic insulin-resistant subjects.¹⁴

The ABCG5 ABCG8 (G5G8) heterodimer functions as a xenobiotic transporter that opposes the absorption of phytosterols and their accumulation in plasma and tissues in both mice and humans.¹⁵ G5G8 also promotes cholesterol secretion into bile and the intestinal lumen.^{16,17} Although its relative contribution to intestinal cholesterol elimination remains unclear, G5G8 accounts for 70% to 90% of biliary cholesterol secretion.^{16,18} However, it should be noted that alternative pathways can contribute to biliary cholesterol secretion under some conditions.¹⁹⁻²¹ In mice lacking functional G5G8, the prevention of phytosterol accumulation by treatment with EZ, deletion of Niemann-Pick C1-like 1 protein, or feeding a plant sterol-free diet corrects metabolic phenotypes associated with G5G8 deficiency, indicating that compensatory mechanisms overcome the loss of G5G8-dependent biliary and intestinal secretion.²²⁻²⁴ When challenged with a plant sterol-free, high-fat diet, the absence of G5G8 accelerates the development of obesity and insulin resistance and increases hepatic cholesterol, steatosis, and inflammation, thereby revealing an essential role for G5G8 in metabolism, independent of its opposition to phytosterol absorption.²²

The phenotype of obese G5G8-deficient mice was associated with increased eukaryotic initiation factor 2 α (eIF2 α) phosphorylation and upregulation of activating transcription factor (ATF) 4 and tribbles 3 (Trb3), suggesting that endoplasmic reticulum (ER) stress contributes to the accelerated loss of glycemic control and amplified steatosis after high-fat feeding. ER stress has been linked to the development of insulin resistance and the

upregulation of lipogenesis in genetically obese leptin-deficient (*ob/ob*) mice.^{25,26} Mice lacking either leptin (*ob/ob*) or its receptor (*db/db*) are hyperphagic, insulin-resistant, and develop severe hepatic steatosis.²⁷ Both strains are also characterized by reduced G5G8 protein and biliary cholesterol, but whether reduced G5G8 deficiency contributes to either ER stress or hepatic phenotypes of either strain is not known.^{28–30}

We hypothesized that increased G5G8-mediated biliary cholesterol secretion would alleviate metabolic phenotypes in genetically obese mice in which G5G8 activity is compromised. Adenoviral vectors encoding G5G8 (AdG5G8) were used to accelerate biliary cholesterol secretion in *db/db* mice. After AdG5G8 delivery, plasma glucose and triglycerides (TGs) were reduced and glucose tolerance was improved. These changes were associated with decreased expression of lipogenic genes, increased Akt phosphorylation, and reduced eIF2 α signaling, suggesting that G5G8-mediated biliary cholesterol secretion alleviates ER stress and restores insulin signaling. However, steatosis was not reduced in this short-term experiment. Additional studies in which stable expression of G5G8 is achieved will be required to determine whether accelerated biliary cholesterol secretion can improve hepatic steatosis in models of obesity and insulin resistance.

Materials and Methods

Materials and Methods are available in the online-only Supplement.

Results

Biliary Cholesterol Elimination

We have previously used adenoviral vectors to transiently increase G5G8 and biliary cholesterol.³¹ Before initiating studies in *db/db* mice, we conducted a pilot study to confirm that AdG5G8 could increase fecal sterol output during the planned treatment period. Fecal neutral sterols increase within 2 days and remain elevated for 6 days after AdG5G8 delivery (Figure I in the online-only Data Supplement). Obese (*db/db*) mice and their lean littermates were injected with a cocktail of adenoviral particles encoding ABCG8 and an empty vector (control) or both ABCG5 and ABCG8 (AdG5G8), and tissues were dissected 3 days after viral delivery. G5 and G8 are obligate heterodimers that require coexpression for complex formation, trafficking to the cell surface, and biliary cholesterol secretion. Both G5 and G8 contain N-linked glycans and heterodimer formation, and trafficking to the cell surface can be monitored by the appearance of the mature, post-Golgi forms of both proteins by SDS-PAGE and immunoblot analysis.³² The immature form of recombinant G8 is observed in all mice, but the mature form is only observed in mice receiving the G5 adenovirus (Figure 1A). Similarly, the mature form of recombinant G5 is only observed in AdG5G8-injected mice that express functional G5G8. AdG5G8 did not increase intestinal levels of the G5G8 transporter, nor did viral cocktails differentially affect liver enzymes or the expression of inflammatory genes in liver (Figure II in the online-only Data Supplement).

We next measured biliary cholesterol and fecal neutral sterols as indirect measures of G5G8 function. AdG5G8 increased biliary cholesterol concentrations in both lean and obese mice

by 5.2-fold and 5.7-fold, respectively (Figure 1B). We also blotted for the class B, type 1 scavenger receptor because this protein can mediate G5G8-independent biliary cholesterol secretion.²⁰ Class B, type 1 scavenger receptor is reduced in *db/db* mice compared with lean controls but is not elevated in either lean or *db/db* mice after AdG5G8 treatment (Figure 1A). The overall ANOVA indicated a significant increase in fecal neutral sterols in AdG5G8-injected mice, regardless of the genotype ($P<0.01$). Post hoc analysis indicated 4.4-fold and 2.9-fold increases in lean and obese mice, respectively. Although levels of G5G8 protein are lower in *db/db* mice compared with lean controls, biliary cholesterol and fecal neutral sterol levels increase to a similar extent.

Glycemic Control, Hepatic ER Stress, and Insulin Signaling

We previously reported that the absence of G5G8 accelerates the loss of glycemic control in high-fat-fed mice.²² To determine whether increased G5G8 and accelerated biliary cholesterol secretion could restore glycemic control in *db/db* mice, we measured fasting glucose and conducted a glucose tolerance test. Overexpression of G5G8 had no effect on fasting glucose in lean mice, nor did it alter glucose disposal in glucose tolerance tests. AdG5G8 decreased plasma fasting glucose in *db/db* mice to levels that were similar to lean controls (Figure 2A). AdG5G8 decreased plasma glucose at 30 and 60 minutes after glucose administration (Figure 2B). There was also a significant reduction in the mean area under the curve for blood glucose in *db/db* mice treated with AdG5G8 compared with control virus (Figure 2B, inset).

We next evaluated hepatic insulin signaling. Livers from *db/db* mice were collected 15 minutes after administration of insulin and subjected to SDS-PAGE and immunoblot analysis. There was an increase in tyrosine-phosphorylated insulin receptor and a decrease in serine-phosphorylated insulin receptor substrate 1 (Figure 2C and 2D), indicating improvements in hepatic insulin sensitivity. An insulin tolerance test revealed a decrease in the area under the curve for blood glucose, but fasting insulin was only modestly lower in AdG5G8-treated mice and failed to reach statistical significance (Figure 2E and 2F).

The loss of glycemic control and hepatic phenotypes in obese G5G8-deficient mice were associated with increased activation of some components of the unfolded protein response (UPR), in particular phosphorylation of eIF2 α .²² Therefore, we determined whether AdG5G8 reduced phospho-eIF2 α and suppressed other components of the UPR in livers of *db/db* mice. Immunoblot analysis demonstrated a reduction in phospho-eIF2 α but not in total eIF2 α in AdG5G8-treated obese mice compared with control virus (Figure 3A and 3B). The reduction in phospho-eIF2 α was associated with less ATF4 mRNA expression and its downstream target, Trb3 (Figure 3C). Trb3 is a negative regulator of insulin-mediated Akt phosphorylation in liver.³³ The decrease in Trb3 was associated with an increase in phospho-Akt but not total Akt, suggesting that alleviation of ATF4-Trb3 signaling plays a role in the restoration of insulin signaling in the livers of AdG5G8-treated *db/db* mice.

To further investigate UPR signaling, we blotted for total and phosphorylated c-Jun N-terminal kinase and pancreatic eIF2 α kinase (PERK). Consistent with reduced ER stress, phospho-c-Jun N-terminal kinase declined after AdG5G8 administration. However, we did not observe elevations in phospho-PERK. In addition, other components of the UPR are

largely unaffected in *db/db* mice treated with AdG5G8 compared with control virus. This includes expression of the ATF6 target genes glucose-regulated protein (GRP) 78, GRP94, CCAAT-enhancer-binding proteins (C/EBP)-homologous protein, and X box-binding protein 1. However, we did detect a modest but significant reduction in spliced X box-binding protein 1, consistent with reduced inositol-requiring enzyme 1 activation. Collectively, these data support a role for accelerated biliary cholesterol secretion in the reduction of eIF2 α signaling, but the kinase and initiating events remain to be resolved.

Plasma and Hepatic Lipids

We broadly assessed changes in genes related to insulin signaling in *db/db* mice using pooled RNA from animals infected with either control virus or AdG5G8 and analyzed by an insulin signaling pathway polymerase chain reaction array (Figure III in the online-only Data Supplement). The majority of genes assayed were unaltered, but key genes in both the lipogenic and gluconeogenic pathways were suppressed, including the lipogenic transcription factor, sterol regulatory-binding protein (SREBP) 1. We confirmed suppression of mRNAs for SREBP1 and its target genes acetyl coenzyme A carboxylase and fatty acid synthase by reverse-transcriptase polymerase chain reaction in individual mice (Figure 4A). Consistent with the reduction in mRNA, full-length SREBP1 protein was lower after AdG5G8 delivery (Figure 4B and 4C). There was also a tendency toward lower levels of cleaved SREBP in nuclear extracts. However, there was no difference in hepatic TG levels 72 hours after AdG5G8 treatment in either lean or *db/db* mice (Figure 4D). We next measured plasma TGs and TG secretion rates (Figure 4E and 4F). TGs were normalized in *db/db* mice, and the TG secretion rate was reduced (542 ± 31 versus 428 ± 23 mg/dL per hour; $P<0.01$) after AdG5G8 administration in *db/db* mice. However, levels of apolipoprotein B (ApoB) and microsomal TG transfer protein mRNAs were unchanged (not shown).

Despite elevations in biliary and fecal sterols, plasma cholesterol was paradoxically increased after AdG5G8 administration in both lean and obese mice (Figure 5A). Fast protein liquid chromatography fractionation of pooled serum revealed that the increase in cholesterol was caused by the accumulation of large particles. High-density lipoprotein levels, which are characteristically elevated in *db/db* mice, declined in both genotypes. A significant fraction of biliary cholesterol is reabsorbed in the small intestine. Therefore, we tested the hypothesis that the unexpected increase in plasma cholesterol after AdG5G8 administration could be averted by coadministration of the cholesterol absorption inhibitor, EZ. In a separate cohort of lean strain-matched mice, we pretreated mice with EZ before administration of control or AdG5G8 virus. As in lean and *db/db* littermates, AdG5G8 increased plasma cholesterol and promoted the accumulation of large cholesterol ester-enriched particles but not in mice in which intestinal absorption was inhibited by pretreatment with EZ (Figure 5C and 5D). Immunoblot analysis of peak fractions revealed that these particles are enriched in both ApoB and ApoE (Figure 5E). Although there is a tendency toward the accumulation of ApoE in whole serum, this difference did not reach statistical significance, and ApoE mRNA was not increased in either liver or intestine (Figure IV in the online-only Data Supplement).

Hepatic cholesterol also increased in *db/db*AdG5G8-treated mice, but unlike plasma cholesterol this was not observed in their lean littermates (Figure 6A). Next, we measured the expression of genes involved in cholesterol synthesis and uptake. Irrespective of viral administration, mRNA levels of SREBP2, 3-hydroxy-3-methylglutaryl-coenzyme A reductase, and 3-hydroxy-3-methylglutaryl-coenzyme A synthase 1 were reduced in *db/db* mice compared with lean controls. Conversely, very-LDLR mRNA levels, which are normally very low in liver, are significantly elevated. In lean mice, AdG5G8 resulted in increased expression of genes required for cholesterol synthesis, suggesting that hepatic cholesterol synthesis increased to maintain hepatic sterol levels in response to accelerated biliary secretion. This effect was not observed in *db/db* mice presumably because of the accumulation of cholesterol in liver. Protein levels of 3-hydroxy-3-methylglutaryl-coenzyme A reductase and LDLR were determined in liver lysates from *db/db* mice (Figure 6). Although there was a trend for increases, neither reached statistical significance.

Discussion

The major findings of the present study are that increased G5G8-mediated biliary cholesterol secretion restores glycemic control, improves hepatic insulin signaling, and reduces plasma triglycerides in obese and insulin-resistant *db/db* mice. These phenotypic differences were associated with reduced markers of ER stress and increased measures of insulin signaling in liver. The abundance of mRNAs for lipogenic genes was reduced, but AdG5G8 failed to lower hepatic lipid content during the 3-day treatment period. Whether sustained expression of G5G8 and accelerated biliary cholesterol secretion during a longer period would promote clearance of hepatic TGs will require alternative approaches to transient expression by adenoviral gene delivery.

G5G8 and the UPR

This study is the converse of our previous work showing that the absence of G5G8 exacerbates the development of insulin resistance, steatosis, and inflammation in diet-induced obesity.²² In the previous study, the development of hepatic insulin resistance was associated with an increase in eIF2 α signaling and reduced phospho-Akt. Consistent with this pathway playing a causative role in hepatic insulin resistance in G5G8-deficient mice, the overexpression of G5G8 in *db/db* mice reduced eIF2 α signaling and increased phospho-Akt. An interesting feature of UPR activation in G5G8 deficiency and its alleviation by AdG5G8 is that it is largely limited to the PERK arm of the UPR. The prevailing model for activation of the UPR is the release of inositol-requiring enzyme 1 (IRE1), ATF6, and PERK from GRP78 by the accumulation of misfolded and unfolded proteins. Although there is some evidence for selective activation of UPR signaling, it is important to note that multiple stress-activated kinases can phosphorylate eIF2 α .^{34,35} In addition, we detected no evidence for reduced phosphoPERK. Consequently, the specificity may have nothing to do with selective activation of the UPR but is rather an alternate mechanism for activating eIF2 α . In addition, a recent report indicates that PERK and inositol-requiring enzyme 1 are responsive to changes in membrane lipid composition, independently of changes in protein folding in the ER.³⁶ Whether membrane cholesterol content similarly affects UPR signaling is not known. The question of how G5G8 influences UPR signaling remains unresolved in

the present study because we have yet to mechanistically link the absence of G5G8 to activation of a specific eIF2 α kinase or other element of the UPR.

ER stress and the UPR are also thought to play a direct role in the upregulation of lipogenesis in leptin-deficient mice.²⁵ In these studies, suppression of the UPR through adenoviral expression of GRP78 represses hepatic lipogenesis and lowers hepatic TGs. Although AdG5G8 reduced plasma TGs and lipogenic gene expression, this was not sufficient to reduce hepatic lipids. These differences may be a matter of degree in which GRP78 more strongly represses lipogenesis or could be because of the disruptions in cholesterol homeostasis associated with AdG5G8. We did not observe changes in GRP78 after AdG5G8 administration in obese mice; the effect of GRP78 and the alleviation of ER stress by this mechanism on G5G8 and biliary cholesterol secretion are yet to be determined.

Leptin and G5G8

In both *ob/ob* and *db/db* mice, G5G8 protein levels are post-transcriptionally reduced and can be increased by caloric restriction or the administration of molecular chaperones. This suggests that reductions in G5G8 are independent of leptin signaling and that ER stress may directly affect G5G8 abundance.³⁰ Perhaps this is not surprising given the dependence of G5G8 formation on lectin chaperones within the ER.³⁷ Conversely, neither diabetes mellitus nor obesity alone is sufficient to reduce hepatic G5G8.³⁰ We recently evaluated another model of obesity and insulin resistance for abundance of G5G5 at the protein level: LDLR-deficient mice maintained on a high-fat, high-cholesterol, Western-type diet for 16 weeks. In this model, G5 protein levels are increased because of the activation of liver X receptor by high-cholesterol diet (Figure V in the online-only Data Supplement). Thus, destabilization of hepatic G5G8 seems to be a feature of obesity limited to genetic models that lack a functional leptin axis. In addition, the upregulation of G5G8 and increased biliary cholesterol secretion may play a protective role in the insulin-resistant liver. Consistent with this idea, ablation of hepatic insulin signaling through liver-specific deletion of insulin receptor increases G5G8 mRNA in a forkhead box O1A–dependent manner.³⁸

G5G8 and Cholesterol Homeostasis

The increase in plasma cholesterol levels after AdG5G8 administration in *db/db* mice was unexpected. The ability of EZ to block this effect of AdG5G8 indicates that this is most likely because of intestinal reabsorption of cholesterol from enriched bile. An enterohepatic pool of cholesterol has been described and is thought to expand during the development of obesity in mice.³⁹ The apparent expansion of this pool of cholesterol resulted in perturbations of plasma and hepatic cholesterol homeostasis that are difficult to unravel and are beyond the scope of the present study. However, this observation highlights the fact that accelerating biliary cholesterol secretion is ineffective in reducing plasma cholesterol unless there is a concomitant increase in intestinal G5G8 or other secretory mechanisms to oppose reabsorption. Similar observations were made in transgenic mice. A liver-specific G5G8 transgene was ineffective in reducing plasma cholesterol or atherosclerosis in the absence of EZ, whereas a human G5G8 transgene under the control of the endogenous promoter that drives expression in both liver and intestine can reduce cholesterol and atherosclerosis.^{40,41}

The primary implication of these findings is that the intestine mitigates the effectiveness of cholesterol elimination by the liver. The role of the intestine in cholesterol elimination has regained attention, with recent studies characterizing transintestinal cholesterol elimination.⁴² Although G5G8 is thought to be responsible for increasing transintestinal cholesterol elimination in response to liver X receptor agonists, there is a G5G8-independent component that is yet to be elucidated.⁴³ Although this pathway can compensate for disruptions in biliary cholesterol elimination, it is not clear how hepatic and intestinal pathways cooperate to maintain cholesterol homeostasis. In this and previous studies in which hepatic cholesterol secretion is significantly elevated, transintestinal cholesterol elimination is insufficient to prevent the reabsorption and accumulation of cholesterol in plasma.

Limitations

The primary limitation of the present study is the use of adenoviral vectors to test the effect of increased G5G8-mediated biliary cholesterol elimination. These vectors dramatically increase protein expression that peaks between 48 and 72 hours after administration and then declines at a rate that is largely dependent on the half-life of the recombinant protein. In the present study, we cannot account for the simultaneous increase in fecal, biliary, hepatic, and plasma cholesterol in AdG5G8-administered *db/db* mice. Several possibilities exist that include mobilization from extrahepatic tissues, such as adipose, or extrahepatic synthesis. Alternatively, there may have been a robust, transient increase in hepatic synthesis followed by repression as cholesterol accumulates in liver. Given the dynamic nature of adenoviral-mediated gene expression, mice are unlikely to achieve steady state. Consequently, studies to evaluate the efficacy of accelerated biliary cholesterol elimination on hepatic steatosis will require approaches that result in sustained increases in G5G8 expression. Such approaches will also facilitate examination of other features of NAFLD such as inflammation and apoptosis.

Supplementary Material

Refer to Web version on PubMed Central for supplementary material.

Acknowledgments

We thank Dr Victoria King (University of Kentucky) for liver samples from low-density lipoprotein receptor-deficient mice.

Sources of Funding

This work was funded by grants from the National Institute of Diabetes and Digestive and Kidney Diseases (to G.A. Graf: R01DK080874) and the National Institute of General Medical Sciences (8 P20 GM103527-05) of the National Institutes of Health.

Nonstandard Abbreviations and Acronyms

AdG5G8	adenoviral vectors encoding G5G8
Apo B	apolipoprotein B

ATF	activating transcription factor
eIF2α	eukaryotic initiation factor 2 α
ER	endoplasmic reticulum
EZ	ezetimibe
G5G8	ABCG5 ABCG8 sterol transporter
GRP	glucose-regulated protein
LDLR	low-density lipoprotein receptor
NAFLD	nonalcoholic fatty liver disease
PERK	pancreatic eIF2 α kinase
SREBP	sterol regulatory element-binding protein
Trb3	tribbles 3
UPR	unfolded protein response

References

1. Savard C, Tartaglione EV, Kuver R, Haigh WG, Farrell GC, Subramanian S, Chait A, Yeh MM, Quinn LS, Ioannou GN. Synergistic interaction of dietary cholesterol and dietary fat in inducing experimental steatohepatitis. *Hepatology*. 2013; 57:81–92. [PubMed: 22508243]
2. Subramanian S, Goodspeed L, Wang S, Kim J, Zeng L, Ioannou GN, Haigh WG, Yeh MM, Kowdley KV, O'Brien KD, Pennathur S, Chait A. Dietary cholesterol exacerbates hepatic steatosis and inflammation in obese LDL receptor-deficient mice. *J Lipid Res*. 2011; 52:1626–1635. [PubMed: 21690266]
3. Van Rooyen DM, Larter CZ, Haigh WG, Yeh MM, Ioannou G, Kuver R, Lee SP, Teoh NC, Farrell GC. Hepatic free cholesterol accumulates in obese, diabetic mice and causes nonalcoholic steatohepatitis. *Gastroenterology*. 2011; 141:1393–1403. 1403.e1. [PubMed: 21703998]
4. Deushi M, Nomura M, Kawakami A, Haraguchi M, Ito M, Okazaki M, Ishii H, Yoshida M. Ezetimibe improves liver steatosis and insulin resistance in obese rat model of metabolic syndrome. *FEBS Lett*. 2007; 581:5664–5670. [PubMed: 18022391]
5. Zheng S, Hoos L, Cook J, Tetzloff G, Davis H Jr, van Heek M, Hwa JJ. Ezetimibe improves high fat and cholesterol diet-induced non-alcoholic fatty liver disease in mice. *Eur J Pharmacol*. 2008; 584:118–124. [PubMed: 18329014]
6. Ushio M, Nishio Y, Sekine O, Nagai Y, Maeno Y, Ugi S, Yoshizaki T, Morino K, Kume S, Kashiwagi A, Maegawa H. Ezetimibe prevents hepatic steatosis induced by a high-fat but not a high-fructose diet. *Am J Physiol Endocrinol Metab*. 2013; 305:E293–E304. [PubMed: 23715726]
7. Muraoka T, Aoki K, Iwasaki T, Shinoda K, Nakamura A, Aburatani H, Mori S, Tokuyama K, Kubota N, Kadowaki T, Terauchi Y. Ezetimibe decreases SREBP-1c expression in liver and reverses hepatic insulin resistance in mice fed a high-fat diet. *Metabolism*. 2011; 60:617–628. [PubMed: 20673929]
8. Altmann SW, Davis HR Jr, Zhu LJ, Yao X, Hoos LM, Tetzloff G, Iyer SP, Maguire M, Golovko A, Zeng M, Wang L, Murgolo N, Graziano MP. Niemann-Pick C1 Like 1 protein is critical for intestinal cholesterol absorption. *Science*. 2004; 303:1201–1204. [PubMed: 14976318]
9. Davis HR Jr, Zhu LJ, Hoos LM, Tetzloff G, Maguire M, Liu J, Yao X, Iyer SP, Lam MH, Lund EG, Detmers PA, Graziano MP, Altmann SW. Niemann-Pick C1 Like 1 (NPC1L1) is the intestinal phytosterol and cholesterol transporter and a key modulator of whole-body cholesterol homeostasis. *J Biol Chem*. 2004; 279:33586–33592. [PubMed: 15173162]

10. Jia L, Ma Y, Rong S, Betters JL, Xie P, Chung S, Wang N, Tang W, Yu L. Niemann-Pick C1-Like 1 deletion in mice prevents high-fat diet-induced fatty liver by reducing lipogenesis. *J Lipid Res.* 2010; 51:3135–3144. [PubMed: 20699423]
11. Jia L, Ma Y, Liu G, Yu L. Dietary cholesterol reverses resistance to diet-induced weight gain in mice lacking Niemann-Pick C1-Like 1. *J Lipid Res.* 2010; 51:3024–3033. [PubMed: 20601625]
12. Umemoto T, Subramanian S, Ding Y, Goodspeed L, Wang S, Han CY, Teresa AS, Kim J, O'Brien KD, Chait A. Inhibition of intestinal cholesterol absorption decreases atherosclerosis but not adipose tissue inflammation. *J Lipid Res.* 2012; 53:2380–2389. [PubMed: 22956784]
13. Park H, Shima T, Yamaguchi K, Mitsuyoshi H, Minami M, Yasui K, Itoh Y, Yoshikawa T, Fukui M, Hasegawa G, Nakamura N, Ohta M, Obayashi H, Okanoue T. Efficacy of long-term ezetimibe therapy in patients with nonalcoholic fatty liver disease. *J Gastroenterol.* 2011; 46:101–107. [PubMed: 20658156]
14. Tsunoda T, Nozue T, Yamada M, Mizuguchi I, Sasaki M, Michishita I. Effects of ezetimibe on atherogenic lipoproteins and glucose metabolism in patients with diabetes and glucose intolerance. *Diabetes Res Clin Pract.* 2013; 100:46–52. [PubMed: 23369229]
15. Sabeva NS, Liu J, Graf GA. The ABCG5 ABCG8 sterol and phytosterols: implications for cardiometabolic disease. *Curr Opin Endocrinol Diabetes Obes.* 2009; 16:172–177. [PubMed: 19306529]
16. Klett EL, Lu K, Kusters A, et al. A mouse model of sitosterolemia: absence of Abcg8/sterolin-2 results in failure to secrete biliary cholesterol. *BMC Med.* 2004; 2:5. [PubMed: 15040800]
17. van der Veen JN, van Dijk TH, Vrins CL, van Meer H, Havinga R, Bijsterveld K, Tietge UJ, Groen AK, Kuipers F. Activation of the liver X receptor stimulates trans-intestinal excretion of plasma cholesterol. *J Biol Chem.* 2009; 284:19211–19219. [PubMed: 19416968]
18. Yu L, Hammer RE, Li-Hawkins J, Von Bergmann K, Lutjohann D, Cohen JC, Hobbs HH. Disruption of Abcg5 and Abcg8 in mice reveals their crucial role in biliary cholesterol secretion. *Proc Natl Acad Sci U S A.* 2002; 99:16237–16242. [PubMed: 12444248]
19. Groen A, Kunne C, Jongsma G, van den Oever K, Mok KS, Petruzzelli M, Vrins CL, Bull L, Paulusma CC, Oude Elferink RP. Abcg5/8 independent biliary cholesterol excretion in Atp8b1-deficient mice. *Gastroenterology.* 2008; 134:2091–2100. [PubMed: 18466903]
20. Wiersma H, Gatti A, Nijstad N, Oude Elferink RP, Kuipers F, Tietge UJ. Scavenger receptor class B type I mediates biliary cholesterol secretion independent of ATP-binding cassette transporter g5/g8 in mice. *Hepatology.* 2009; 50:1263–1272. [PubMed: 19637290]
21. Coy DJ, Wooton-Kee CR, Yan B, Sabeva N, Su K, Graf G, Vore M. ABCG5/ABCG8-independent biliary cholesterol excretion in lactating rats. *Am J Physiol Gastrointest Liver Physiol.* 2010; 299:G228–G235. [PubMed: 20413720]
22. Su K, Sabeva NS, Liu J, Wang Y, Bhatnagar S, van der Westhuyzen DR, Graf GA. The ABCG5 ABCG8 sterol transporter opposes the development of fatty liver disease and loss of glycemic control independently of phytosterol accumulation. *J Biol Chem.* 2012; 287:28564–28575. [PubMed: 22715101]
23. Yu L, von Bergmann K, Lutjohann D, Hobbs HH, Cohen JC. Ezetimibe normalizes metabolic defects in mice lacking ABCG5 and ABCG8. *J Lipid Res.* 2005; 46:1739–1744. [PubMed: 15930515]
24. Tang W, Ma Y, Jia L, Ioannou YA, Davies JP, Yu L. Genetic inactivation of NPC1L1 protects against sitosterolemia in mice lacking ABCG5/ABCG8. *J Lipid Res.* 2008; 50:293–300. [PubMed: 18796403]
25. Kammoun HL, Chabanon H, Hainault I, Luquet S, Magnan C, Koike T, Ferré P, Foufelle F. GRP78 expression inhibits insulin and ER stress-induced SREBP-1c activation and reduces hepatic steatosis in mice. *J Clin Invest.* 2009; 119:1201–1215. [PubMed: 19363290]
26. Ozcan U, Yilmaz E, Ozcan L, Furuhashi M, Vaillancourt E, Smith RO, Görgün CZ, Hotamisligil GS. Chemical chaperones reduce ER stress and restore glucose homeostasis in a mouse model of type 2 diabetes. *Science.* 2006; 313:1137–1140. [PubMed: 16931765]
27. Larter CZ, Yeh MM. Animal models of NASH: getting both pathology and metabolic context right. *J Gastroenterol Hepatol.* 2008; 23:1635–1648. [PubMed: 18752564]

28. Tran KQ, Graewin SJ, Swartz-Basile DA, Nakeeb A, Svatek CL, Pitt HA. Leptin-resistant obese mice have paradoxically low biliary cholesterol saturation. *Surgery*. 2003; 134:372–377. [PubMed: 12947343]
29. Bouchard G, Johnson D, Carver T, Paigen B, Carey MC. Cholesterol gallstone formation in overweight mice establishes that obesity per se is not linked directly to cholelithiasis risk. *J Lipid Res*. 2002; 43:1105–1113. [PubMed: 12091495]
30. Sabeva NS, Rouse EJ, Graf GA. Defects in the leptin axis reduce abundance of the ABCG5-ABCG8 sterol transporter in liver. *J Biol Chem*. 2007; 282:22397–22405. [PubMed: 17561514]
31. Graf GA, Yu L, Li WP, Gerard R, Tuma PL, Cohen JC, Hobbs HH. ABCG5 and ABCG8 are obligate heterodimers for protein trafficking and biliary cholesterol excretion. *J Biol Chem*. 2003; 278:48275–48282. [PubMed: 14504269]
32. Graf GA, Li WP, Gerard RD, Gelissen I, White A, Cohen JC, Hobbs HH. Coexpression of ATP-binding cassette proteins ABCG5 and ABCG8 permits their transport to the apical surface. *J Clin Invest*. 2002; 110:659–669. [PubMed: 12208867]
33. Du K, Herzig S, Kulkarni RN, Montminy M. TRB3: a tribbles homolog that inhibits Akt/PKB activation by insulin in liver. *Science*. 2003; 300:1574–1577. [PubMed: 12791994]
34. Maiuolo J, Bulotta S, Verderio C, Benfante R, Borgese N. Selective activation of the transcription factor ATF6 mediates endoplasmic reticulum proliferation triggered by a membrane protein. *Proc Natl Acad Sci U S A*. 2011; 108:7832–7837. [PubMed: 21521793]
35. Kilberg MS, Shan J, Su N. ATF4-dependent transcription mediates signaling of amino acid limitation. *Trends Endocrinol Metab*. 2009; 20:436–443. [PubMed: 19800252]
36. Volmer R, van der Ploeg K, Ron D. Membrane lipid saturation activates endoplasmic reticulum unfolded protein response transducers through their transmembrane domains. *Proc Natl Acad Sci U S A*. 2013; 110:4628–4633. [PubMed: 23487760]
37. Graf GA, Cohen JC, Hobbs HH. Missense mutations in ABCG5 and ABCG8 disrupt heterodimerization and trafficking. *J Biol Chem*. 2004; 279:24881–24888. [PubMed: 15054092]
38. Biddinger SB, Haas JT, Yu BB, Bezy O, Jing E, Zhang W, Unterman TG, Carey MC, Kahn CR. Hepatic insulin resistance directly promotes formation of cholesterol gallstones. *Nat Med*. 2008; 14:778–782. [PubMed: 18587407]
39. Roy S, Hyogo H, Yadav SK, Wu MK, Jelicks LA, Locker JD, Frank PG, Lisanti MP, Silver DL, Cohen DE. A biphasic response of hepatobiliary cholesterol metabolism to dietary fat at the onset of obesity in the mouse. *Hepatology*. 2005; 41:887–895. [PubMed: 15793852]
40. Wilund KR, Yu L, Xu F, Hobbs HH, Cohen JC. High-level expression of ABCG5 and ABCG8 attenuates diet-induced hypercholesterolemia and atherosclerosis in *Ldlr*^{-/-} mice. *J Lipid Res*. 2004; 45:1429–1436. [PubMed: 15175362]
41. Basso F, Freeman LA, Ko C, Joyce C, Amar MJ, Shamburek RD, Tansey T, Thomas F, Wu J, Paigen B, Remaley AT, Santamarina-Fojo S, Brewer HB Jr. Hepatic ABCG5/G8 overexpression reduces apoB-lipoproteins and atherosclerosis when cholesterol absorption is inhibited. *J Lipid Res*. 2007; 48:114–126. [PubMed: 17060690]
42. Temel RE, Brown JM. Biliary and nonbiliary contributions to reverse cholesterol transport. *Curr Opin Lipidol*. 2012; 23:85–90. [PubMed: 22262055]
43. van der Velde AE, Vrins CL, van den Oever K, Kunne C, Oude Elferink RP, Kuipers F, Groen AK. Direct intestinal cholesterol secretion contributes significantly to total fecal neutral sterol excretion in mice. *Gastroenterology*. 2007; 133:967–975. [PubMed: 17854600]

Significance

This study demonstrates for the first time that active elimination of cholesterol through the biliary compartment can reduce unfolded protein response signaling, restore glycemic control, and reduce plasma triglycerides in a mouse model of obesity and insulin resistance that is characterized by elevated levels of endoplasmic reticulum stress. These findings add to a growing body of literature that supports a causal role for cholesterol in the development of obesity-related liver phenotypes. It also suggests that therapeutic approaches to actively reduce hepatic cholesterol in the setting of obesity and insulin resistance may provide benefit in the treatment of insulin resistance and nonalcoholic fatty liver disease.

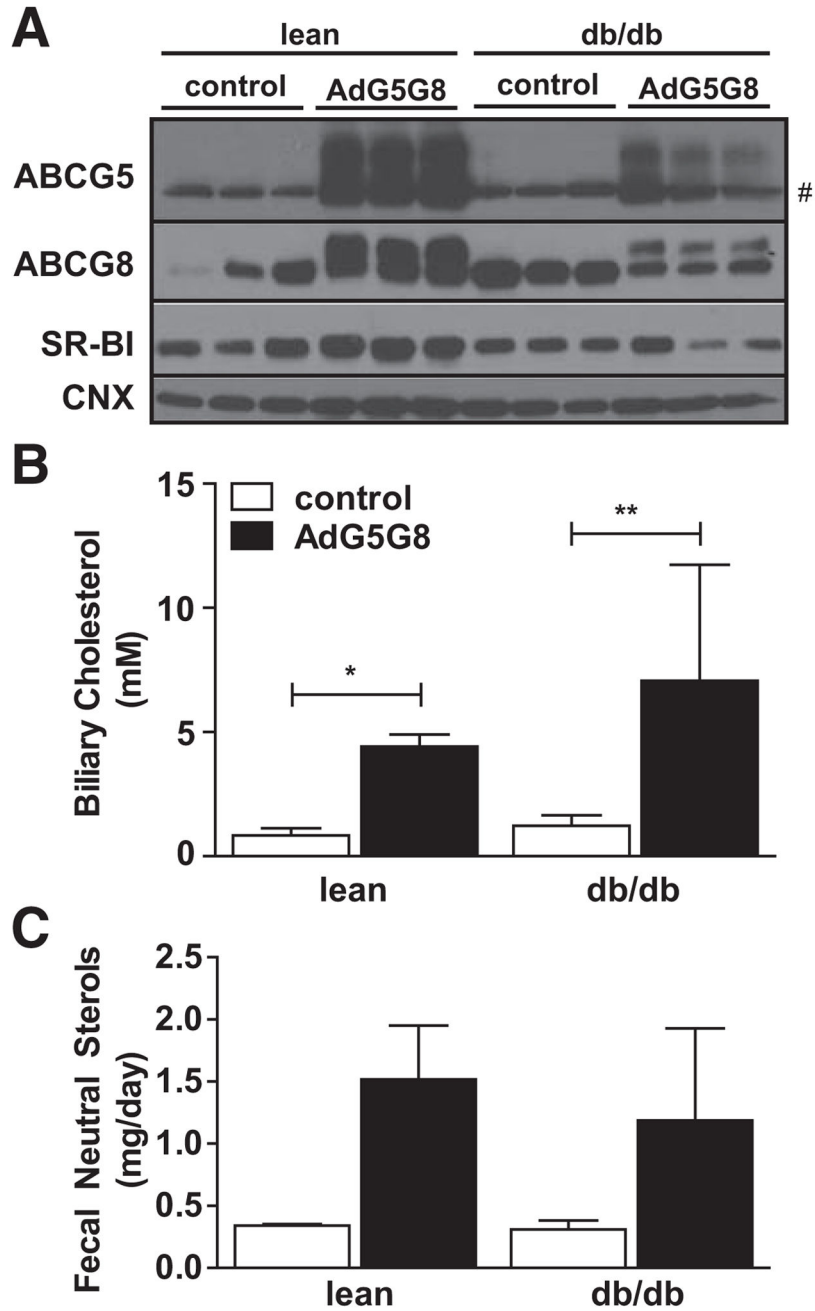


Figure 1.

Adenoviral vectors encoding G5G8 (AdG5G8) increases biliary cholesterol and fecal neutral sterols in lean and obese mice. Obese (*db/db*) male mice and their lean littermates were administered a cocktail of AdG5G8 or empty virus and G8 (control). **A**, Hepatic expression of G5G8 was confirmed by immunoblot analysis. # Appearance of nonspecific band that comigrates with immature G5. Calnexin (CNX) was used as a loading control. **B** and **C**, Biliary cholesterol concentrations and fecal neutral sterols were measured by gas chromatography-mass spectrometry (GC-MS). Data are mean \pm SEM (n=3). Horizontal lines

terminating in vertical bars denote significant difference from control virus within genotype.
* $P < 0.05$, ** $P < 0.01$. SR-BI indicates class B, type 1 scavenger receptor.

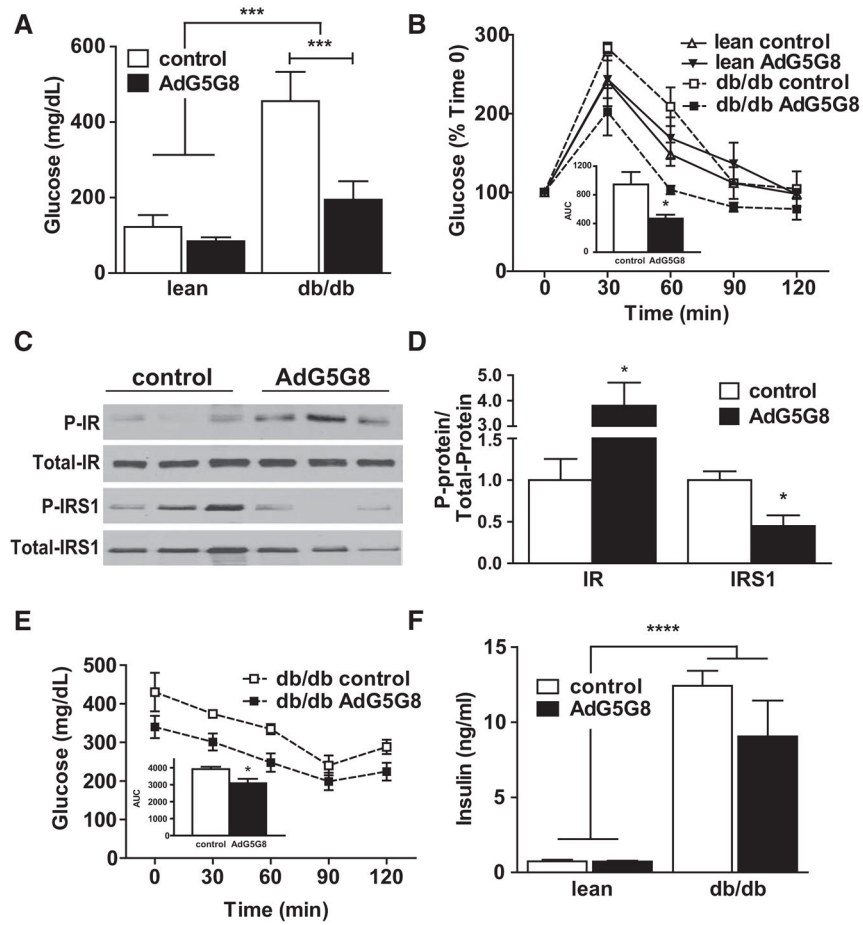


Figure 2.

Adenoviral vectors encoding G5G8 (AdG5G8) improves glycemic control in obese *db/db* mice. Lean and *db/db* mice were administered control and AdG5G8 vectors. **A**, Fasting glucose was determined. **B**, Glucose tolerance test was conducted 72 hours after viral administration. **B** (inset), Areas under the curve were calculated for each individual mouse. **C** and **D**, Immunoblot analysis of total and phosphorylated (P-) insulin receptor (IR) and IR substrate 1 (IRS-1). **E**, An insulin sensitivity test was performed. **F**, Fasting insulin levels were determined in an independent cohort of *db/db* mice. Data are mean±SEM (n=3–6). Horizontal lines terminating in vertical bars denote significant difference from control virus within genotype. * $P < 0.05$, *** $P < 0.001$, **** $P < 0.0001$.

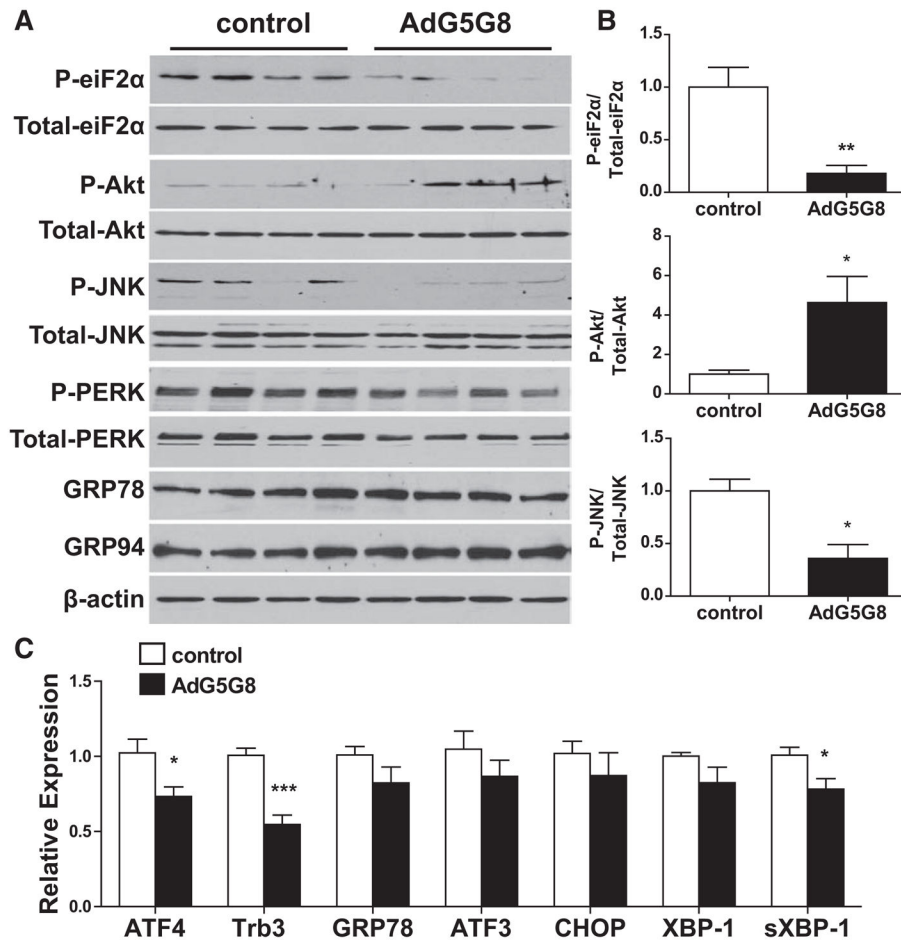


Figure 3. Adenoviral vectors encoding G5G8 (AdG5G8) reduces eukaryotic initiation factor 2 α (eiF2 α) signaling in *db/db* mice. Obese (*db/db*) mice were administered control and AdG5G8 vectors. **A**, Total and phosphorylated (P-) eiF2 α , Akt, c-Jun N-terminal kinase (JNK), and pancreatic eiF2 α kinase (PERK) were assessed in hepatic lysates by SDS-PAGE and immunoblotting. The activating transcription factor (ATF) 6 target genes glucose-regulated protein (GRP) 78 and GRP94 were also assessed. β -actin was used as a loading control. **B**, The ratios of phosphorylated to total eiF2 α , Akt, and JNK were determined by densitometry. **C**, Reverse-transcriptase polymerase chain reaction was used to measure downstream signaling for eiF2 α (ATF4, tribbles 3 [Trb3]), ATF6 (GRP78, X box-binding protein 1 [XBP-1]), and inositol-requiring enzyme 1 (spliced sXbp1). Data are mean \pm SEM (n=4). * P <0.05, ** P <0.01, *** P <0.001. CHOP indicates C/EBP-homologous protein.

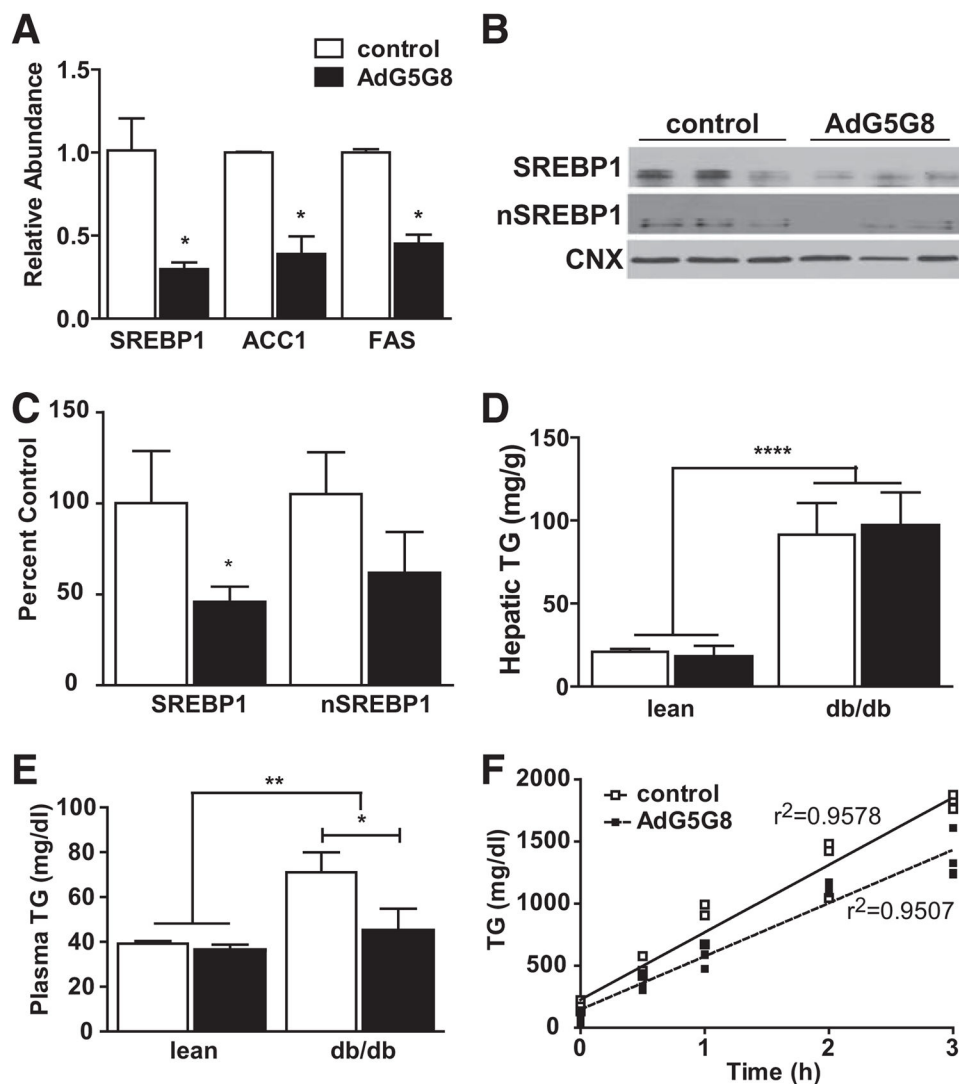


Figure 4. Adenoviral vectors encoding G5G8 (AdG5G8) reduces lipogenic gene expression and lowers plasma triglycerides (TGs). Obese (*db/db*) male mice and their lean littermates were administered control or AdG5G8 virus. **A**, Total RNA was extracted from liver 72 hours after viral administration and was analyzed by reverse-transcriptase polymerase chain reaction for expression of lipogenic genes. **B**, Full-length and processed sterol regulatory element-binding protein (SREBP) 1 were analyzed by immunoblotting in whole cell lysates and nuclear extracts, respectively. **C**, Densitometry of SREBP immunoblots. Signal intensities are normalized to calnexin (CNX) and expressed as percent of the control mean. **D** and **E**, Plasma and hepatic TGs were determined by enzymatic colorimetric assay. **F**, TG secretion rates were determined after injection of Triton WR 1339. Data are mean \pm SEM (n=3–4). * P <0.05, ** P <0.01, **** P <0.0001.

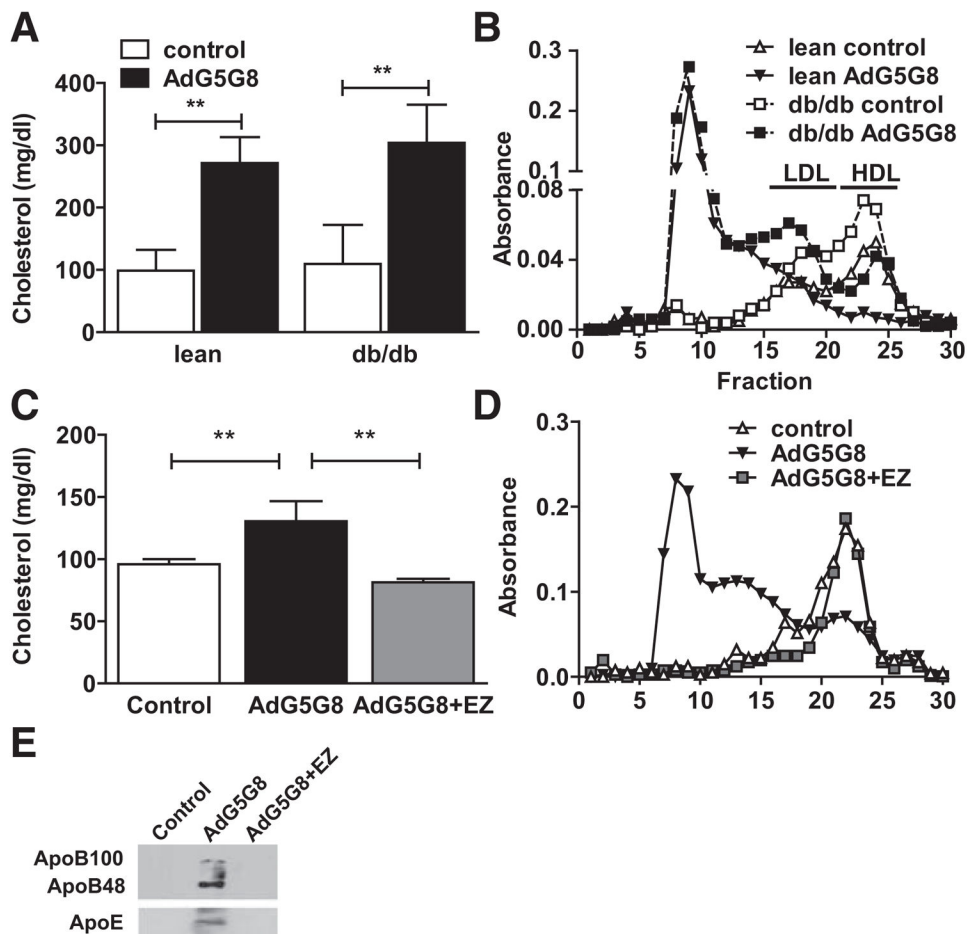


Figure 5. Adenoviral vectors encoding G5G8 (AdG5G8)-dependent increase in plasma cholesterol is blocked by ezetimibe. **A** and **B**, Lean and obese *db/db* mice were administered control and AdG5G8 vectors. **C** and **E**, C57Bl6/J mice were administered the control vector or AdG5G8 in the absence or presence of ezetimibe (AdG5G8+ezetimibe [EZ]). Cholesterol in total (**A** and **C**) and fast protein liquid chromatography (FPLC)-fractionated (**B** and **D**) serum was determined by enzymatic colorimetric assay. **E**, FPLC fraction of 8 samples (peak cholesterol) from 3 mice in each group was pooled and analyzed by immunoblotting for apolipoprotein B (ApoB). HDL indicates high-density lipo-protein; and LDL, low-density lipoprotein.

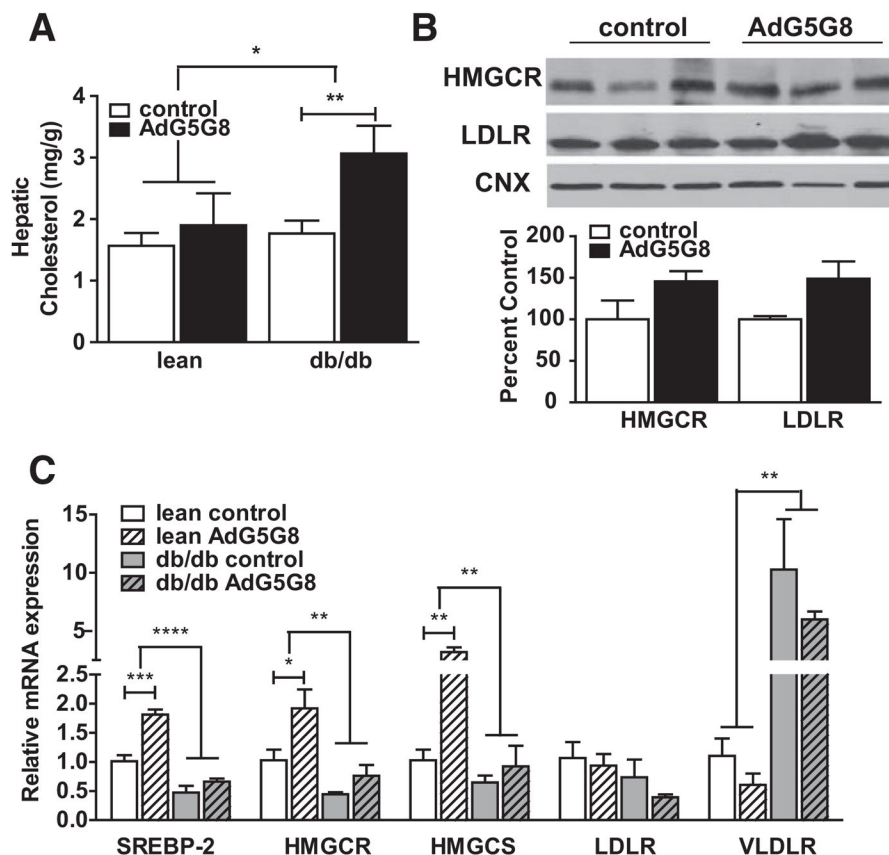


Figure 6. Adenoviral vectors encoding G5G8 (AdG5G8) disrupts hepatic cholesterol homeostasis. Obese *db/db* male mice and their lean littermates were administered control or AdG5G8 virus. **A**, Total hepatic lipids were extracted and cholesterol was measured by enzymatic colorimetric assay and expressed as mg/g wet tissue weight. **B**, Immunoblot and densitometric analysis of hepatic 3-hydroxy-3-methylglutaryl-coenzyme A reductase (HMGCR) and low-density lipoprotein receptor (LDLR). **C**, Total RNA was extracted from liver 72 hours after viral administration and analyzed by reverse-transcriptase polymerase chain reaction for expression of genes involved in cholesterol synthesis and uptake. Data are mean \pm SEM (n=3–4). Horizontal lines terminating in vertical bars denote significant difference from control virus within genotype. * P <0.05, ** P <0.01, *** P <0.001, **** P <0.0001. CNX indicates calnexin; HMGCS, 3-hydroxy-3-methylglutaryl-coenzyme A synthase; SREBP, sterol regulatory element-binding protein; and VLDLR, very-LDLR.